

p-CdS/n-Si Anisotype Heterojunction Solar Cells With Efficiency of 6.4%

**Raid A. Ismail¹,
Abdul-Majeed E. Al-Samar'ai²
and Omar A. A. Sultan³**

¹School of Applied Sciences, University of Technology, Baghdad, Iraq

²Department of Physics, College of Education, Al-Mustansiriyah University

³NASSR State Company, Ministry of Industry and Minerals

خلايا شمسية نوع المفرق الهجين p-CdS/n-Si بكفاءة تحويل 6.4%

رائد عبد الوهاب إسماعيل¹
عبد المجيد عيادة السامرائي²
عمر عبد الستار عبد الرزاق سلطان³

¹قسم العلوم التطبيقية - الجامعة التكنولوجية - العراق

²قسم الفيزياء - كلية التربية - الجامعة المستنصرية - العراق

³شركة نصر العامة - وزارة الصناعة والمعادن - العراق

في هذا البحث، تم تصنيع خلايا شمسية من المفرق الهجين p-CdS/n-Si لأول مرة بطريقة الرش الكيميائي الحراري. باستخدام هذه الطريقة المنخفضة الكلفة، تم الحصول على كفاءة تحويل بمقدار 6.4% تحت شروط إضاءة Air Mass 1 وعلى عامل ملئ بمقدار 0.32. أظهرت خصائص تيار-جهد أن سلوك التيار عند الانحياز الأمامي مطابق لميكانيكية الاختراق-إعادة الاتحاد. بينت قياسات الاستجابة الطيفية أن لهذه الخلايا منطقة استجابة طيفية عريضة (400-1150 nm)، وأن منحنى الاستجابة لهذه الخلايا يمتلك قمتين متميزتين: الأولى عند الطول الموجي 550 nm والثانية عند الطول الموجي 800 nm. لقد أوضحت تقنية اضمحلال فولتية الدائرة المفتوحة المحتثة ضوئياً أن فترة حياة الحاملات الأقلية لهذه الخلايا كانت بحدود 20 μm.

Keywords: CdS/Si, Solar Cells, Spray pyrolysis.

ABSTRACT

In the present paper, p-CdS/n-Si heterojunction solar cells are prepared for the first time by the spray pyrolysis technique. Using such low-cost method, cells with 6.4% AM1 conversion efficiency and 0.32 fill factor have been made. The forward current of the prepared cells is dominated by the tunneling-recombination mechanism. Spectral response measurements revealed that these cells exhibit a wide spectral response (400-1150 nm) with two distinct peaks, the first at $\lambda=550\text{nm}$, while the second at $\lambda=800\text{nm}$. Photo-induced open-circuit voltage decay technique illustrated that the minority carriers lifetime of these cells is around $20\mu\text{s}$.

Introduction

There has been considerable interest in recent years directed towards the development of heterojunction solar cells [1-3]. Such interest is based on the fact that heterojunction devices have a number of advantages over diffused p-n junction solar cells include [4]: (i) a lower junction-formation temperature, (ii) higher spectral response at short wavelengths, and (iii) many of deposited layers have the right indices of refraction to act as antireflection coating. CdS/Si and In-doped CdS/Si heterojunction solar cells have been reported to have power conversion efficiencies of 4% and greater [5-8]. The CdS films in these devices are deposited by different methods. Most of these films are deposited by either evaporation or sputtering in a vacuum and post-deposition heat treatments are necessary. However, no attempt is reported for depositing CdS onto Si by chemical spray pyrolysis technique yet. In this letter, we report the preliminary results of the first fabrication of p-CdS/n-Si heterojunction solar cells made by chemical spray pyrolysis technique. Preliminary aspects of this work have been reported earlier [9,10].

Experimental Procedures

Single-crystal silicon wafers of n-type with (111) orientation are used as substrates, they have a resistivity in the range of 1-5 $\Omega\text{-cm}$, and one face of the wafer is polished to the mirror-like surface. Prior to deposition of CdS, the wafers were chemically etched in dilute hydrofluoric acid to remove native oxides. Then back contact metallization was accomplished by vacuum depositing 200 nm layer of Al. Subsequently, after removal from the vacuum chamber, the wafers were scribed into individual pieces of 0.5cm^2 sizes, then they were sent to spraying apparatus. The deposition of CdS films was carried out by spraying an aqueous solution of CdCl_2 and thiourea onto a heated silicon substrate maintained at 450°C . A typical spray mixture, which gave us good results, consists of an 0.2 M solution of cadmium salt and 0.2 M solution of thiourea. This solution is sprayed in a deposition rate of about 2nm/s . After the deposition of CdS, frontal metal electrode is a 200nm layer of Al through a metal mask. The sensitive area was about 0.2cm^2 . The optical transmittance of the CdS thin films prepared on glass substrates was measured using (UV/VIS-PV-8800) spectrophotometer covering the range 400-900 nm. Spectral responsivity measurements of CdS/Si heterojunction solar cells were made by using a monochromator (MODEL 746) in the range 400-1100 nm (the spectrum of interest in the operation of solar cells under terrestrial applications). The results were calibrated by measuring the power of each spectral line using a standard power meter. (J-V) measurements were done under dark and illuminated conditions. The illumination was achieved under simulated AM1 condition (93 mW/cm^2) by a halogen lamp type "PHILIPS"; 120 W, which connected to a Variac and calibrated by a silicon powermeter. The type of conductivity of CdS film was determined by using Hall measurement. The minority carrier lifetime of the cells was

measured by the photo-induced Open Circuit Voltage Decay technique (OCVD). The experimental set-up of the OCVD technique can be found elsewhere [9].

Results and Discussion

The transmittance of CdS thin films as a function of wavelength is shown in Figure 1. It is seen that the transmittance of CdS film is higher at higher substrate temperature (T_{sb}), this is easily interpreted as follows: rising T_{sb} causes a decrease in the thickness of the deposited films due to the increase in sublimation rate [10, 11].

Figure 1 also shows an increase in transmittance with wavelength, attains the value 550 nm wavelength (the absorption edge of CdS 2.4 eV), then slightly increase is observed beyond this value. CdS films exhibit a high transparency in the region from about 550 nm, (about 70%), i.e. CdS film represents window layer for such spectral region.

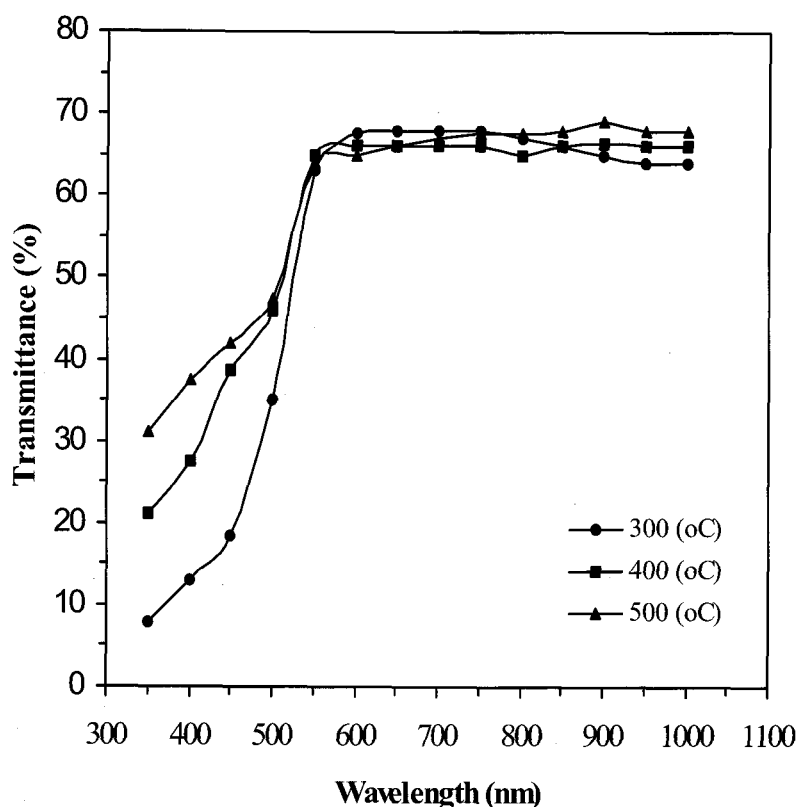


Figure 1. Spectral Transmittance for CdS Films prepared at Different Glass T_{sb} .

Figure 2 presents a relative spectral response of the cells fabricated. It is noted that the responsivity curve shows good band-pass behavior (window effect), and it is comprised of four distinct regions, the first region (corresponding to the blue spectral region) shows an increase in responsivity with wavelength, attains the maximum value at $\lambda=550$ nm (the absorption edge of the CdS frontal layer). The lower responsivity at the shorter wavelength region may be due to the absorption of the light near the surface (shallow absorption depth), which has large amount of surface recombination of the photogenerated carriers, the second region of the plot shows a decrease in responsivity with a minimum value at $\lambda=600$ nm, this could be attributed to a high degree of carrier recombination at

the interface [12], the third region shows an increase in the responsivity passing through the maximum value at $\lambda=800$ nm corresponding to light absorption at transition region on silicon side. The fourth region shows that responsivity decreases reaching the absorption edge of the silicon 1.1eV. The smaller responsivity at longer wavelength is ascribed to the carriers generated deep in the bulk of the silicon [13].

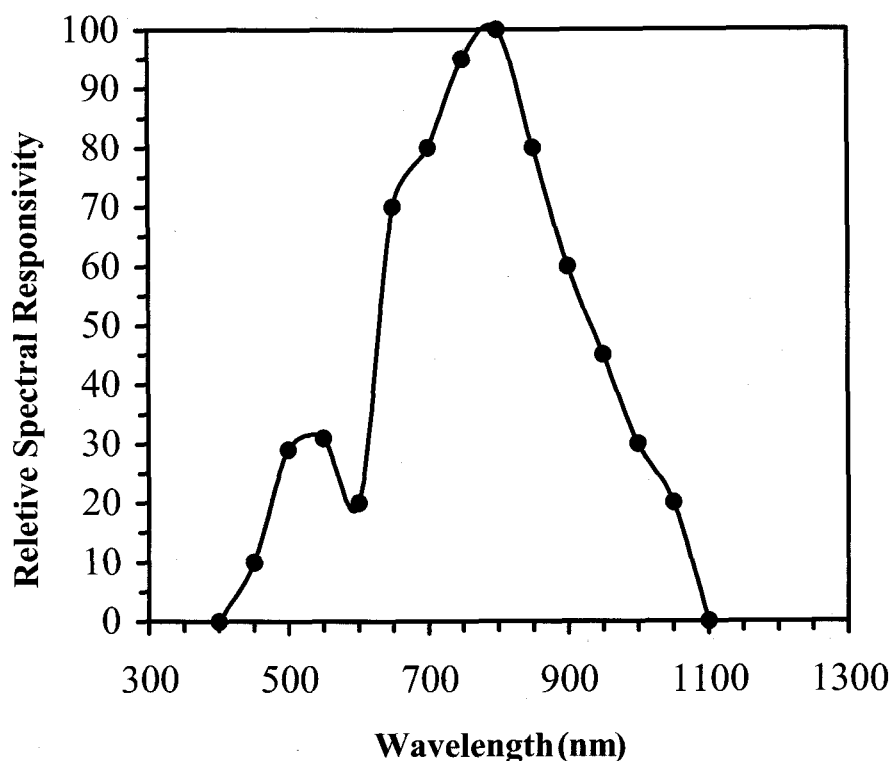


Figure 2. Relative Spectral Responsivity Curve of CdS/n-Si Heterojunction Solar Cells.

Figure 3 shows the dark and illuminated J-V characteristics for a selected cell. The figure reveals the effect of illumination on the J-V plots. The decrease in illumination forward current I_{ph} as compared with the dark forward current I_f is due to the generation of minority carriers, which are annihilated by the majority carriers dark current.

The intersection between the photogenerated and dark forward currents is probably due to the high density of the interfacial states.

The fourth quadrant curve represents the photovoltaic performance in which the power can be generated by the cell. This quadrant predicts a low value of fill factor (poor rectangularity). The measured open circuit voltage V_{OC} given from this curve is 465mV and the measured short circuit current density J_{SC} is 40.5mA/cm². A reasonable interpretation may be obtained from the nature of the dark current under reverse bias, it is a noticeable variation in dark current with reverse bias voltage, and this effect can be attributed to the carrier generation inside the depletion region.

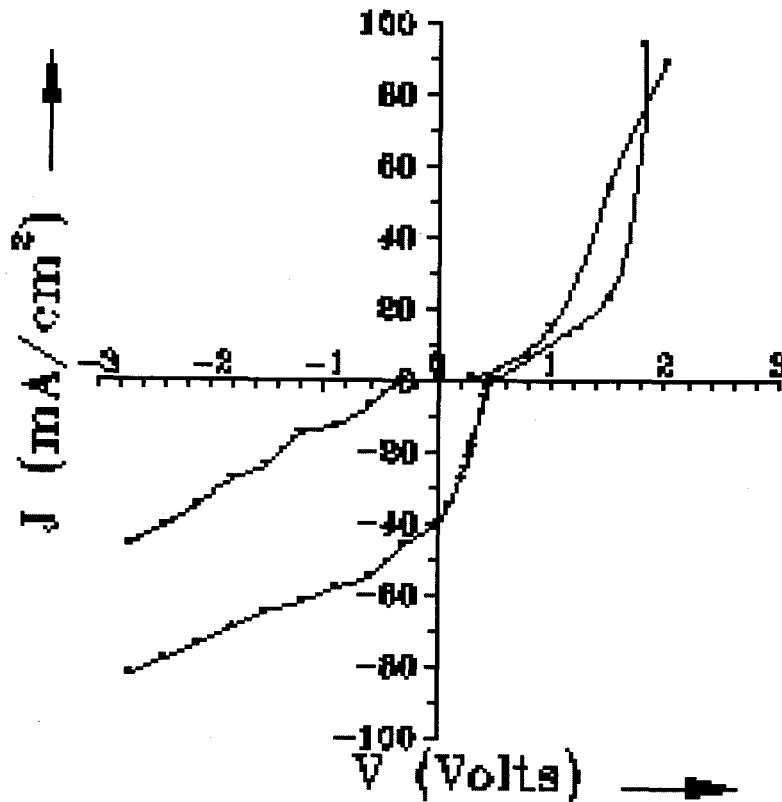


Figure 3. Dark and Illuminated J-V Characteristics under Simulated AM1 Conditions for a Selected Cell.

A semi-log J-V plot under forward bias is presented in Figure 4. This figure shows that forward current consists of two regions. The first one represents the recombination current, while the second region represents the tunneling current, i.e. CdS/n-Si heterojunction obeys to the tunneling-recombination model. This result is not in contradiction with results obtained by other workers for CdS/Si heterojunction prepared by vacuum evaporation [14,15]. The saturation current density of the first region J_{S1} is determined by extrapolating (J-V) curve of this region to find its intercept with $V=0$. Thus, the ideality factor n is calculated by the following equation [16]:

$$n = \frac{q}{kT} \cdot \frac{\partial V}{\partial \ln(I_{f1}/I_{S1})} \quad (1)$$

where q/kT is the reciprocal of the volt equivalent of temperature, I_{f1} is the forward current of the first region. On the other hand, the saturation current density of the second region J_{S2} is determined by the extrapolation at the second region, then the value of A is extracted by the following equation [16]:

$$A = \frac{d \ln(I_{f2}/I_{S2})}{dV} \quad (2)$$

where I_{f2} is the forward current of the second region.

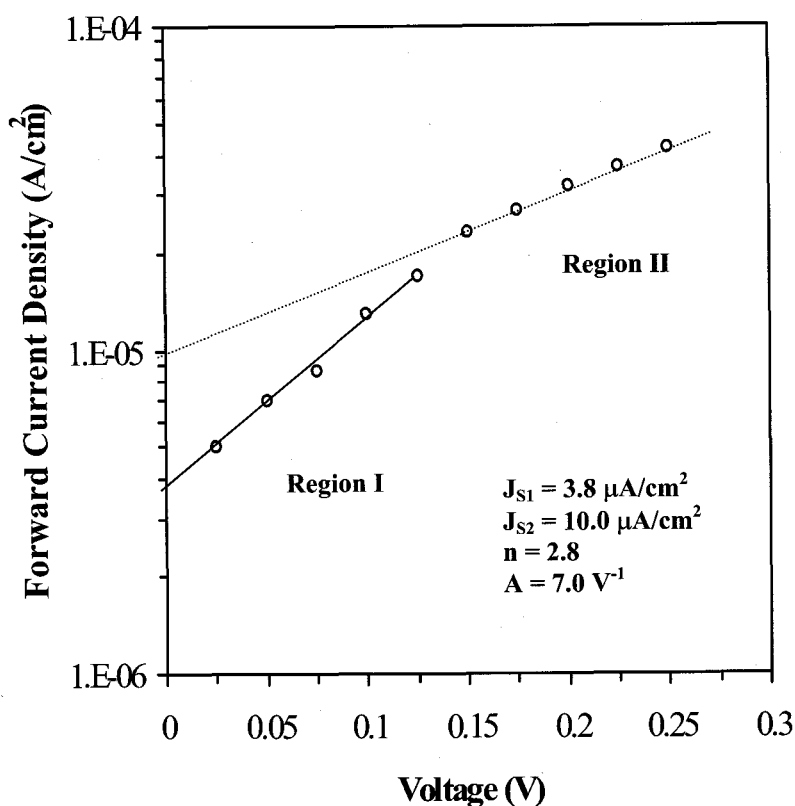


Figure 4. Forward (J-V) Characteristics for CdS/n-Si Heterojunction.

Figure 5 demonstrates the variation of the output power (the power extracted from the cell under simulated AM1) versus voltage across the load resistance. The figure reveals that sprayed CdS/Si heterojunction is a suitable device to produce a high efficient solar cell with a conversion efficiency of 6.45%. The high value of conversion efficiency can be elucidated by the window effect taken place between these combinations. In contrast, the low value of fill factor FF is probably due to oxide formation at the interface [7], which can be avoidable by using inert gas instead of air through the spray process.

A minority carrier lifetime (τ) is an important parameter in solar-cell design. This parameter was measured using (OCVD) technique. The experimental set-up of this technique is presented elsewhere [17]. Since these cells are horizontal-junction devices, the decay mode will correspond to a condition of intermediate injection, where the excess minority carrier concentration in the base is greater than the thermal-equilibrium minority carrier concentration but less than the thermal-equilibrium majority carrier concentration. Under these conditions the minority carrier lifetime can be computed from the following expression [18]:

$$\tau = \frac{kT}{q} \left/ \frac{1}{dV_{OC}/dt} \right/ \quad (3)$$

where t is the decay time.

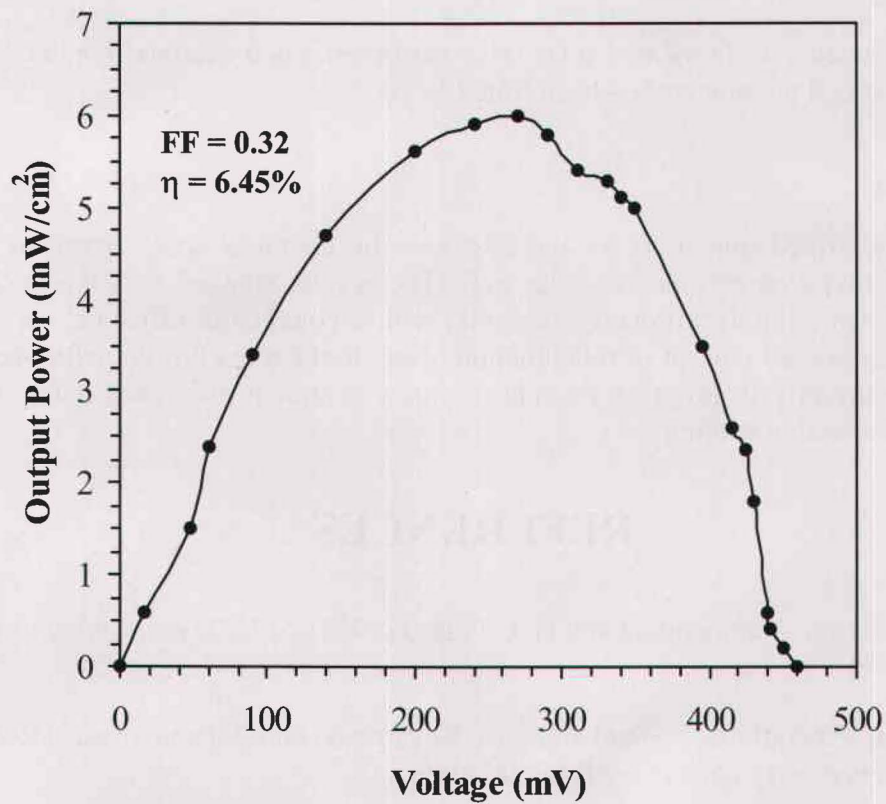


Figure 5. The Variation of the Output Power vs. Voltage across the Load Resistance for CdS/n-Si Heterojunction Solar Cell.



Figure 6. Photo-Induced Open-Circuit Voltage Decay Photograph.

Figure 6 shows a photograph of V_{OC} decay curve. The lifetime was calculated from Eqn. (3) and it was around 20 μ s.

The conversion efficiency of fabricated solar cells was investigated over six months. No significant degradation in solar cell parameters has been found.

Conclusions

CdS films were deposited onto n-Si for the first time by chemical spray pyrolysis technique to introduce the anisotype heterojunction solar cell. The results showed that this technique is an appropriate to fabricate highly efficient solar cells with a conversion efficiency of 6.4% and fill factor of 0.32. The forward current of this junction obeys to the model of tunneling-recombination. Experiments are currently in progress to improve the conversion efficiency using a grid frontal electrode and antireflection coating.

REFERENCES

- [1] S. R. Vishwakarma , Rahmatullah and H. C.Prasad (1993). *Solid State Communications* **85** (12): 1055-1059.
- [2] Georgakilas, E. Aperathitis, V. Fonkaraki, M. Kayambaki and P. Panayototas (1997). *Materials Science and Engineering* **B44**: 383-386.
- [3] E. Sader (2000). *Fourth International Conference on Physics of Condensed Matter*, April 18th-2000, University of Jordan, 185-194.
- [4] Tom Feng, Amal K. Ghosh and Charles Fishman (1979). *Appl. Phys. Lett.* **35** (3): 266-268.
- [5] F. A. Aboufotouh, R. Alawadi and M. M. Abd-Elnaby (1982). *Thin Solid Films* **96**: 169-173.
- [6] E. Scafe`, G. Maletta, R. Tomaciello, P. Alessandrini, A. Camanzi, L. DE Angelis, and F. Galluzi (1988). *Solar Cells* **10**: 17-32.
- [7] F. J. Garcia, A. Ortiz-Conde and A. Sa-Neto (1988). *Appl. Phys. Lett.* **52** (15): 1261-1262.
- [8] Philips Laou (1994). *Dissertation Abstracts*, McGill University, Canada, 1994.MAI 33/04.
- [9] Raid A. Ismail, Abdul-Majeed E. Al-Samar'ai and Omar A. A. Sultan (2000). *Journal of DIALA* No.8, **Part 2**: .87-95.
- [10] M. D. Uplane and S. H. Pawar (1983). *Solid State Communications* **46** (12): 847-850
- [11] M. D. Uplane and S. H. Pawar (1983). *Solar Cells* **10**: 177-187.
- [12] Raid A. Ismail, Abdul-Majeed E. Al-Samar'ai and Omar A. A. Sultan (2000) *J. Al-Rafidain Eng.* **8** (2): 77-83.
- [13] A. G. Milnes and D. L. Feucht (1972). *Heterojunctions and Metal-Semiconductor Junctions*, Academic Press, New York.

- [14] W. Budde (1983). *Optical Radiation Measurements V4*, Academic Press, New York.
- [15] Takasaki, Tomokazu, EMA, Yoshinori, HayashiI, and Toshiya (1986). *Electron Commun. Jpn., Part2*, **69** (3): 39-45.
- [16] Toshikazu Suda and Akio (1983). *Journal of Crystal Growth* **61**: 494-498.
- [17] B. L. Sharma and R. K. Purohit (1974). *Semiconductor Heterojunctions*, Pergamon Press, New York.
- [18] Jonh E. Mahan, Thomas W. Ekstedt, Robert I. Frank and Roy Kaplow (1974). *IEEE Transactions on Electron Devices* **ED-26** (5): 733-739.